

Continuous Variable Entanglement and Squeezing of Orbital Angular Momentum States

M. Lassen^{1,2}, G. Leuchs^{2,3}, and U. L. Andersen¹

¹*Department of Physics, Technical University of Denmark, Fysikvej, 2800 Kgs. Lyngby, Denmark*

²*Max Planck Institute for the Science of Light, Günther Scharowskystrasse 1, 91058 Erlangen, Germany*

³*University Erlangen-Nürnberg, Staudtstrasse 7/B2, 91058 Erlangen, Germany.*

(Dated: May 20, 2022)

We report the first experimental characterization of the first-order continuous variable orbital angular momentum states. Using a spatially non-degenerate optical parametric oscillator (OPO) we produce quadrature entanglement between the two first-order Laguerre-Gauss modes. The family of OAM modes is mapped on an orbital Poincare sphere, and the modes position on the sphere is spanned by the three orbital parameters. Using the non-degenerate OPO we produce squeezing of these parameters, and as an illustration, we reconstruct the "cigar-shaped" uncertainty volume on the orbital Poincare sphere.

PACS numbers: 42.50.-p; 03.67.-a; 42.50.Dv

Propagating light beams have a spin angular momentum and an orbital angular momentum (OAM), which are associated with the polarization and the phase distribution of the light state, respectively [1]. The *quantum* spin angular momentum (or polarization) has been thoroughly investigated both for single photons and for continuous variables [2, 3, 4]; for example polarization entanglement has been created and utilized for various quantum information protocols. Recently the *quantum* OAM of light has also attracted a lot of attention, especially in the single photon regime due to its unique capabilities in tailoring the dimensionality of the Hilbert space [5, 6, 7]. In contrast, there has been very little work devoted to the OAM of modes described by continuous variables; the only account in this regime is the very recent work on the creation of CV entanglement between two spatially separated OAM modes generated in atomic vapor exploiting the non-linear process of four-wave-mixing [8, 9]. OAM of single photons has already found uses in various quantum information protocol, and we envisage that the CV OAM states hold similar potentials. The most promising application of CV OAM states is their connectivity with atoms, thus allowing for storage of CV quantum information [10, 11].

The simplest spatial mode that can carry OAM is the first order Laguerre-Gaussian (LG) mode which produce either a left-handed or right-handed corkscrew-like phase front and a ring-structured intensity profile. They are denoted $LG_{p=0}^{l=\pm 1}$, where l and p are the azimuthal and radial mode indices. Similarly to quantum spin angular momentum (polarization) states, the family of first-order OAM states can be represented on a Poincare-sphere analog which is also known as the first-order orbital Poincare sphere [12, 13]. The sphere is spanned by three parameters (associated with three different OAM states of light) that have properties identical to those of the three polarization Stokes parameters and which we name the orbital parameters. In this paper we demonstrate the generation of squeezing in the orbital parameter of OAM modes using a spatially non-degenerate optical parametric oscillator

and a specially tailored local oscillator. In addition, we measure quadrature entanglement between the two first-order LG modes thereby demonstrating a new type of entanglement from non-degenerate OPOs.

The quantum polarization degree of freedom (or spin angular momentum) has been extensively explored and characterized in the Schwinger representation in terms of the quantum Stokes operators both in the two-dimensional and the infinite-dimensional Hilbert space, where the Stokes parameter eigenvalues are either discrete or continuous [2, 3, 4]. The Stokes operators are decomposed into field operators for orthogonal polarization modes and completely represent the quantum dynamics of the polarization of light. Likewise, we define the Stokes operator analogs - the orbital operators - for the first order OAM modes as

$$\begin{aligned}\hat{O}_1 &= \hat{A}_{HG_{10}}^\dagger \hat{A}_{HG_{10}} - \hat{A}_{HG_{01}}^\dagger \hat{A}_{HG_{01}} \\ \hat{O}_2 &= \hat{A}_{HG_{10(45^\circ)}}^\dagger \hat{A}_{HG_{10(45^\circ)}} - \hat{A}_{HG_{10(135^\circ)}}^\dagger \hat{A}_{HG_{10(135^\circ)}} \\ \hat{O}_3 &= \hat{A}_{LG_0^{+1}}^\dagger \hat{A}_{LG_0^{+1}} - \hat{A}_{LG_0^{-1}}^\dagger \hat{A}_{LG_0^{-1}},\end{aligned}\quad (1)$$

where \hat{A}^\dagger and \hat{A} are the creation and annihilation operators for the various spatial first-order modes given by the indices, and illustrated on the sphere in Fig. 1. As clearly seen from these definitions, \hat{O}_1 , \hat{O}_2 and \hat{O}_3 represents the difference in the photon number between the two modes HG_{10} and HG_{01} , $HG_{10(45^\circ)}$ and $HG_{10(135^\circ)}$, and LG_0^{+1} and LG_0^{-1} , respectively. Similarly to the polarization Stokes operators, these orbital operators completely represent the dynamics of the first-order spatial states, and thus these operators follow the same algebra as the Stokes operators, namely the $SU(2)$ algebra [14]. Likewise, the commutation relations are $[\hat{O}_k, \hat{O}_l] = i\hat{O}_m$ where $k, l, m \in \{1, 2, 3\}$ of cyclic permutation.

Spatially multimode non-classical CV states have previously been generated in pulsed optical parametric amplification [15], in atomic vapor [8], in a confocal optical parametric oscillator [16] and in linear interference be-

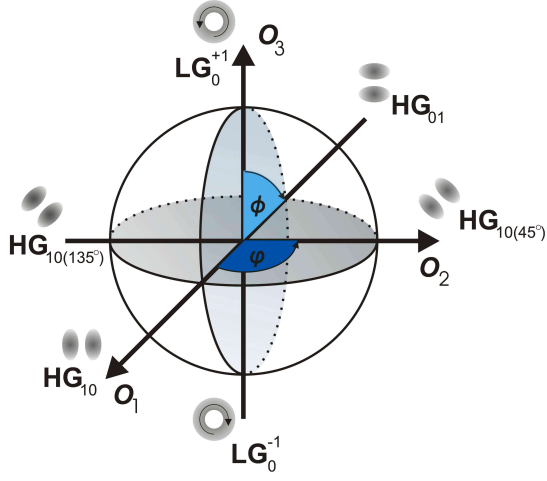


FIG. 1: Orbital Poincare sphere of the first-order OAM modes. Points on the sphere are associated with a superposition of OAM modes [13]: $\psi_{\phi,\varphi} = \cos(\phi/2)LG_0^{+1} + \exp(i\varphi)\sin(\phi/2)LG_0^{-1}$, with azimuthal and axial angles ϕ and φ .

tween different single modes [17, 18, 19]. Here we use another approach that previously has been used for the generation of single-spatial-mode squeezed states, namely a mode-stable (and non-confocal) optical parametric oscillator [20]. By employing a type I phase-matched nonlinear crystal in a mode-stable optical cavity, the polarization, the frequency and the spatial degree of freedom are usually degenerate which lead to single mode quadrature squeezing as demonstrated by various groups. In all these experiments, the cavity supported only the Gaussian zero'th order LG mode. However, by changing the cavity resonance frequency it is possible to generate the two first order modes simultaneously due to their frequency degeneracy (stemming from their identical Gouy phase shifts). This means that the down-converted signal and idler photons are produced in two distinct orthogonal spatial modes (the OAM modes, LG_0^{+1} and LG_0^{-1}), and thus creates quadrature entanglement between these two modes similarly to the production of entanglement between polarization modes [21] or between frequency modes [22] in polarization or frequency non-degenerate OPOs. The non-degeneracy of the first-order LG modes therefore adds a new member to the family of non-degenerate OPOs capable of producing entanglement. This was also discussed in ref. [23] for an OPO above the oscillation threshold. In the following, we experimentally demonstrate the generation of quadrature entangled LG modes and show that this can be used to produce squeezing in the first order orbital parameters.

Our experimental setup is depicted in Fig. 2 and besides the laser source it consists of two mode-cleaning cavities (for green and for infrared light (IR)), an OPO, a HG-LG mode converter and a homodyne detection scheme. The laser source (Diabolo from Innolight) de-

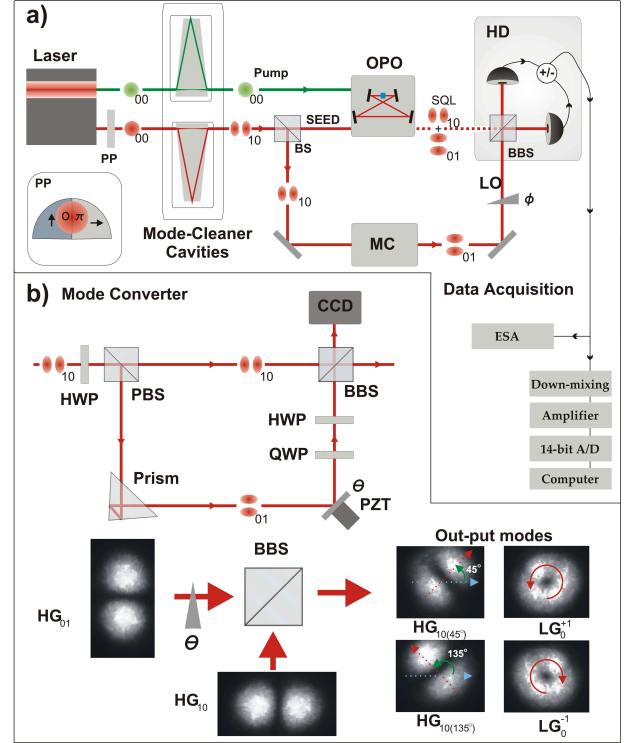


FIG. 2: a) Schematics of the experimental setup to generate amplitude squeezing. b) Mode converter (MC) for the generation of the local oscillator. The interference process in the mode-converted is illustrated and some of the experimentally obtained interference patterns are shown. BBS: Balanced beam splitter (50/50 BS). PBS: Polarizing beam splitter. HWP: $(\lambda/2)$ Half-wave plate. QWP: $(\lambda/4)$ Quarter-wave plate. PZT: Piezo-electrical element for controlling phases. PP: Phase-Plate. The prism rotates the HG modes by 45° .

livers 400 mW of IR (1064 nm) light and 650 mW of green (532 nm) light. The OPO is composed of a bow-tie shaped cavity in which a $1 \times 2 \times 10 \text{ mm}^3$ type I periodically poled KTP crystal (Raicol Inc) is placed in the smallest beam waist. Our cavity consists of two curved mirrors of 25 mm radius of curvature and two plane mirrors. Three of the mirrors are highly reflective at 1064 nm, $R > 99.95\%$, while the output coupler has a transmittance of $T = 8\%$. At the wavelength of the pump beam (532 nm), the transmittance of the mirrors is larger than 95%. Besides the pump beam, the OPO cavity is seeded with a very dim HG_{10} beam at 1064 nm. The spatial profile of this beam has been tailored in the mode-cleaning cavity and to enhance the transmission through the cavity, the Gaussian beam from the laser passes first through a phase-flip plate (PP) which produces a relative phase flip of π between the two halves of the Gaussian beam (and thus mimics the HG_{10} mode) [17]. Seeding the cavity with a HG_{10} mode has a two-fold purpose; one is to enable an active cavity lock at the frequency of the HG_{10} (which coincide with the frequencies of the HG_{01} , LG_0^{+1} and LG_0^{-1} modes), and the other one is to ensure the gen-

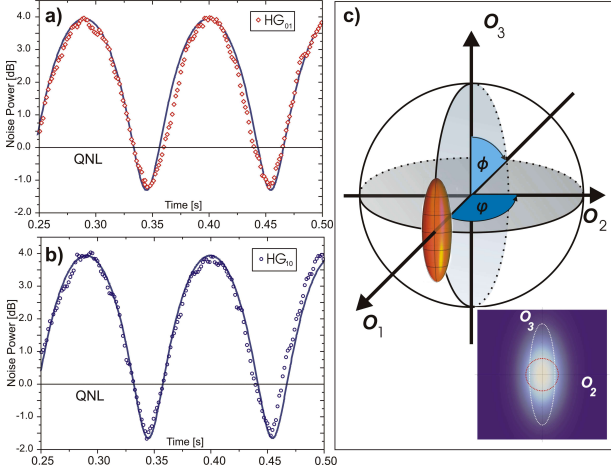


FIG. 3: Experimental squeezing traces for the a) HG_{01} and b) HG_{10} modes, where the relative phase between the LO and the squeezed beam is scanned. The traces are recorded with a ESA. Resolution bandwidth of 300 kHz and a video bandwidth of 300 Hz at a detection frequency of 5.5 MHz. We measured -1.6 ± 0.2 dB of squeezing and $+4.0 \pm 0.2$ dB of anti-squeezing for the HG_{10} mode, -1.4 ± 0.2 dB of squeezing and $+4.1 \pm 0.2$ dB of anti-squeezing for the HG_{01} mode. These values have been corrected for electrical noise, which is 12 ± 0.2 dB below the QNL and is mostly due to the amplifiers in the photo-detectors. c) Illustration of the uncertainty volume on the orbital Poincare sphere and associated with the orbital parameters. The relative elongation of the volume is based on the measured values (however its size relative to the sphere is not in scale). The projection on the O_2 - O_3 plane is also shown.

eration of squeezing of the HG_{10} with a small coherent excitation (less than 1 mW). Although the ideal spatial profile of the pump beam for down conversion efficiency optimization is a superposition of $HG_{00}+HG_{20/02}$ mode for the $HG_{10/01}$, we have chosen to use a Gaussian mode for simplicity reasons, and the resulting decrease in efficiency is overcome by using a more intense beam. The relative phase between the pump and seed is locked to de-amplification of the seed beam, thus generating amplitude squeezing.

To proof the existence of quadrature entanglement between the two LG modes, we measure the quadrature quantum noise of the spatial modes in a rotated basis composed of the first order HG modes, HG_{10} and HG_{01} : By performing a simple basis transformation from the LG modes to HG modes, it is easy to show that $\hat{X}_{HG_{10}} = (\hat{X}_{LG_0^{-1}} + \hat{X}_{LG_0^{+1}})/\sqrt{2}$ and $\hat{X}_{HG_{01}} = (\hat{P}_{LG_0^{-1}} - \hat{P}_{LG_0^{+1}})/\sqrt{2}$, where \hat{X} and \hat{P} are the amplitude and phase quadratures of the modes denoted by the lower indices. According to the criterion of Duan et al. [24] and Simon [25], CV entanglement can be witnessed if

$$V(\hat{X}_{LG_0^{+1}} + \hat{X}_{LG_0^{-1}}) + V(\hat{P}_{LG_0^{+1}} - \hat{P}_{LG_0^{-1}}) < 2, \quad (2)$$

where $V(\dots)$ is the variance. Using the transformation,

the criterion reduces to $V(\hat{X}_{HG_{10}}) + V(\hat{X}_{HG_{01}}) < 2$, and thus by measuring the amplitude quadrature variances of the two HG modes, entanglement between the OAM modes can be witnessed.

The quadrature variances of the HG modes are analyzed using balanced homodyne detection (HD) with a spatially tailored Local Oscillator (LO) mode, which is either a HG_{10} or a HG_{01} mode depending on which signal mode is measured. We produce the HG_{10} LO using the mode cleaning cavity as described above, and the HG_{01} LO is generated by converting the HG_{10} mode using a prism. The outcomes of the HD is fed into a spectrum analyzer which is set to display the noise power (corresponding to the second moment) of the signal beam at 5.5 MHz with a bandwidth of 300kHz (and 300 Hz averaging). We first calibrate the shot noise limit, the result of which is illustrated in Fig. 3 by the horizontal lines. Next we measure the noise traces for the HG_{10} and HG_{01} modes while the phase of the LOs are scanned, see Fig. 3. All data are normalized to the shot noise level. By fitting the measured data to a theoretical squeezing curve, we find amplitude quadrature squeezing of -1.6 ± 0.2 dB and -1.4 ± 0.2 dB for the HG_{10} and HG_{01} mode, respectively (corresponding to the minima of the curves). Inserting these values into the entanglement criterion we find $V(X_{HG_{10}}) + V(X_{HG_{01}}) = 1.42 < 2$.

The measured squeezing values are degraded by the various inefficiencies of our setup. We estimate this efficiency to be $\eta_{total} = \eta_{cav}\eta_{prop}\eta_{det}\eta_{hd}$, where $\eta_{prop} = 0.97 \pm 0.02$ is the propagation efficiency, $\eta_{det} = 0.90 \pm 0.05$ is the photo-detector (Epitaxx ETX500) efficiency, $\eta_{cav} = 0.94$ is the cavity escape efficiency and $\eta_{hd} = 0.96 \pm 0.02$ is the spatial overlap efficiency in the homodyne detector. The total estimated detection efficiencies for our experiment is therefore $\eta_{total} = 0.79 \pm 0.04$. From these efficiencies can we infer the following squeezing values: -2.2 ± 0.2 dB and -1.9 ± 0.2 dB for the HG_{10} and HG_{01} modes, respectively, and the entanglement criterion is $V(X_{HG_{10}}) + V(X_{HG_{01}}) = 1.25 < 2$. We thus have proven that the spatially non-degenerate OPO produces quadrature entanglement between the first order OAM modes.

We now proceed by characterizing the variances of the orbital parameters that defines the position of the state on the orbital Poincare sphere. First we note that the orbital parameters can be linearized for our setup by decomposing the field operators into a part representing the coherent excitation and a part representing the quantum noise; $\hat{A}_{HG_{01}} = \langle \hat{A}_{HG_{01}} \rangle + \delta \hat{A}_{HG_{01}}$ and $\hat{A}_{HG_{10}} = \langle \hat{A}_{HG_{10}} \rangle + \delta \hat{A}_{HG_{10}}$, and noting that $\langle \hat{A}_{HG_{01}} \rangle = 0$ and $\langle \hat{A}_{HG_{10}} \rangle \neq 0$:

$$\begin{aligned} \delta \hat{O}_1 &= \langle \hat{A}_{HG_{HG_{10}}} \rangle^2 \delta \hat{X}_{HG_{10}} \\ \delta \hat{O}_2 &= \langle \hat{A}_{HG_{HG_{10}}} \rangle^2 \delta \hat{X}_{HG_{01}} \\ \delta \hat{O}_3 &= \langle \hat{A}_{HG_{HG_{10}}} \rangle^2 \delta \hat{P}_{HG_{01}}, \end{aligned} \quad (3)$$

where we have used the definitions $\delta \hat{X} = \hat{A} + \delta \hat{A}^\dagger$ and $\delta \hat{P} = -i(\delta \hat{A} - \delta \hat{A}^\dagger)$. We see that in the regime where

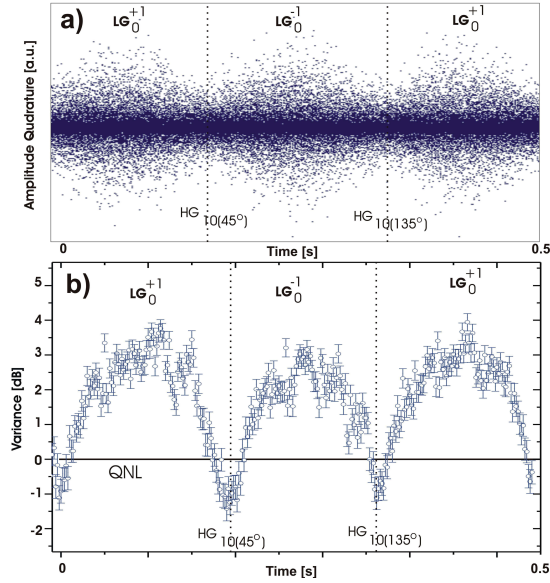


FIG. 4: a) Time trace for the amplitude quadrature for spatial modes along a ring on the orbital Poincare sphere spanned by \hat{O}_2 and \hat{O}_3 . b) Amplitude quadrature variances for the various spatial modes on the ring.

linearization is valid, the orbital operators are linear functions of the amplitude and phase quadratures of different spatial modes. Therefore, the precision in determining first-order spatial modes depends on the quadrature noise of the light modes. For example, for a bright excitation in the HG_{10} mode, as in our case, its determination on the sphere is given by the noise in the orthogonal orbital plane spanned by \hat{O}_2 and \hat{O}_3 corresponding to the quadrature noise of the HG_{01} mode (see eq. 3). The quadrature variances of this mode is given in Fig. 3b. Moreover the variance of \hat{O}_1 is given by the variance of the amplitude quadrature of the HG_{10} mode given by the minimum squeezing value in Fig. 3b. Based on these measurements we may define a cigar-shaped uncertainty

volume on the orbital Poincare sphere associated with first-order OAM state as illustrated in Fig. 3c.

Full tomographic reconstruction of the first-order OAM state is also possible by measuring all possible projections on the sphere using spatially tailored local oscillator modes (similarly to the tomographic reconstruction of the polarization state [26]). Some modes of the LO are made by interfering equally intense HG_{10} and HG_{01} modes with a continuous varying relative phase shift, as shown in Fig. 2b. By matching these LO modes with the OAM modes, we measure the amplitude quadratures of the modes along a ring on the orbital sphere, thus mapping out the quadrature noise of a whole family of different OAM states. The results of the amplitude quadrature measurements are shown in Fig. 4a for a 150 kHz broad signal at 5.5 MHz. We also compute the variance of these data as depicted in Fig. 4b. In particular, we observe a very large variance in the LG modes which is a signature of entanglement as measured above.

To conclude, we have generated a new quantum state of light composed of quadrature entangled LG modes. For the generation we used an OPO operating in a new regime where all field parameters are degenerate except for its spatial degree of freedom for which it is two-fold degenerate. The produced OAM states from the OPO are mapped on an orbital Poincare sphere which is similar to the standard Poincare sphere for polarization. We generate a classically bright HG_{10} mode described on this sphere but its exact location is determined by the noise of the orthogonal HG_{01} dark mode. As this dark state was quadrature squeezed from the OPO, we have demonstrated squeezing in the orbital parameters defining the position of the mode on the orbital Poincare sphere. In addition we have measured the noise of the bright orbital parameter and thereby reconstructed the uncertainty volume of the first-order OAM state.

We acknowledge the financial support from the EU (COMPAS) and the Danish Research Council (FTP). ML acknowledge support from the Alexander von Humboldt Foundation.

-
- [1] L. Allen *et al.*, Phys. Rev. A **45**, 8185 (1992).
 - [2] A. S. Chirkin *et al.*, Quantum Electron **23**, 870 (1993).
 - [3] N. Korolkova *et al.*, Phys. Rev. A **65**, 052306 (2002).
 - [4] W. P. Bowen *et al.*, Phys. Rev. Lett. **88**, 093601 (2002).
 - [5] N. K. Langford *et al.*, Phys. Rev. Lett. **93**, 053601 (2004).
 - [6] S. P. Walborn *et al.*, Phys. Rev. A **71**, 053812 (2005).
 - [7] A. Mair *et al.*, Nature **412**, 313 (2001).
 - [8] V. Boyer *et al.*, Phys. Rev. Lett. **100**, 143601 (2008).
 - [9] V. Boyer *et al.*, Science **321**, 544 (2008).
 - [10] R. Inoue, N. Kanai, T. Yonehara, Y. Miyamoto, M. Koashi and M. Kosuma, Phys. Rev. A **74**, 053809 (2006).
 - [11] D.V. Vasilyev, I. V. Sokolov and E. S. Polzik, Phys. Rev. A **77**, 020302 (2008).
 - [12] M. J. Padgett and J. Courtial, Opt. Lett. **24**, 430 (1999).
 - [13] G. F. Calvo, Opt. Lett. **30**, 1207 (2005).
 - [14] G. S. Agarwal, J. Opt. Soc. Am. A **16**, 2914 (1999).
 - [15] S.-K. Choi *et al.*, Phys. Rev. Lett. **83**, 1938 (1999).
 - [16] M. Martinelli *et al.*, Phys. Rev. A **67**, 023808 (2003).
 - [17] N. Treps *et al.*, Phys. Rev. Lett., **88**, 203601 (2002).
 - [18] M. Lassen *et al.*, Phys. Rev. Lett. **98**, 083602 (2007).
 - [19] K. Wagner *et al.*, Science **321**, 5888, 541 (2008).
 - [20] L.A. Wu *et al.*, Phys. Rev. Lett. **57**, 691 (1986).
 - [21] Z. Y. Ou, S. F. Pereira, H. J. Kimble, and K. C. Peng, Phys. Rev. Lett. **68**, 3663 (1992).
 - [22] A.S. Villar *et al.*, Phys. Rev. Lett. **95**, 243603 (2005).
 - [23] C. Navarrete-Benlloch *et al.*, Phys. Rev. Lett. **100**, 203601 (2008).
 - [24] L.M. Duan *et al.*, Phys. Rev. Lett. **84**, 2722 (2000).
 - [25] R. Simon, Phys. Rev. Lett. **84**, 2726 (2000).
 - [26] Ch. Marquardt *et al.*, Phys. Rev. Lett. **99**, 220401 (2007).